

On the Molecular Origin of Photoluminescence of Nonblinking Carbon Dot

Ananya Das, Venkatesh Gude, Debjit Roy, Tanmay Chatterjee, Chayan K. De, and Prasun K. Mandal*

Department of Chemical Sciences, Indian Institute of Science Education and Research (IISER) Kolkata, Mohanpur, West-Bengal, 741246, India. e-mail: prasunchem@iiserkol.ac.in

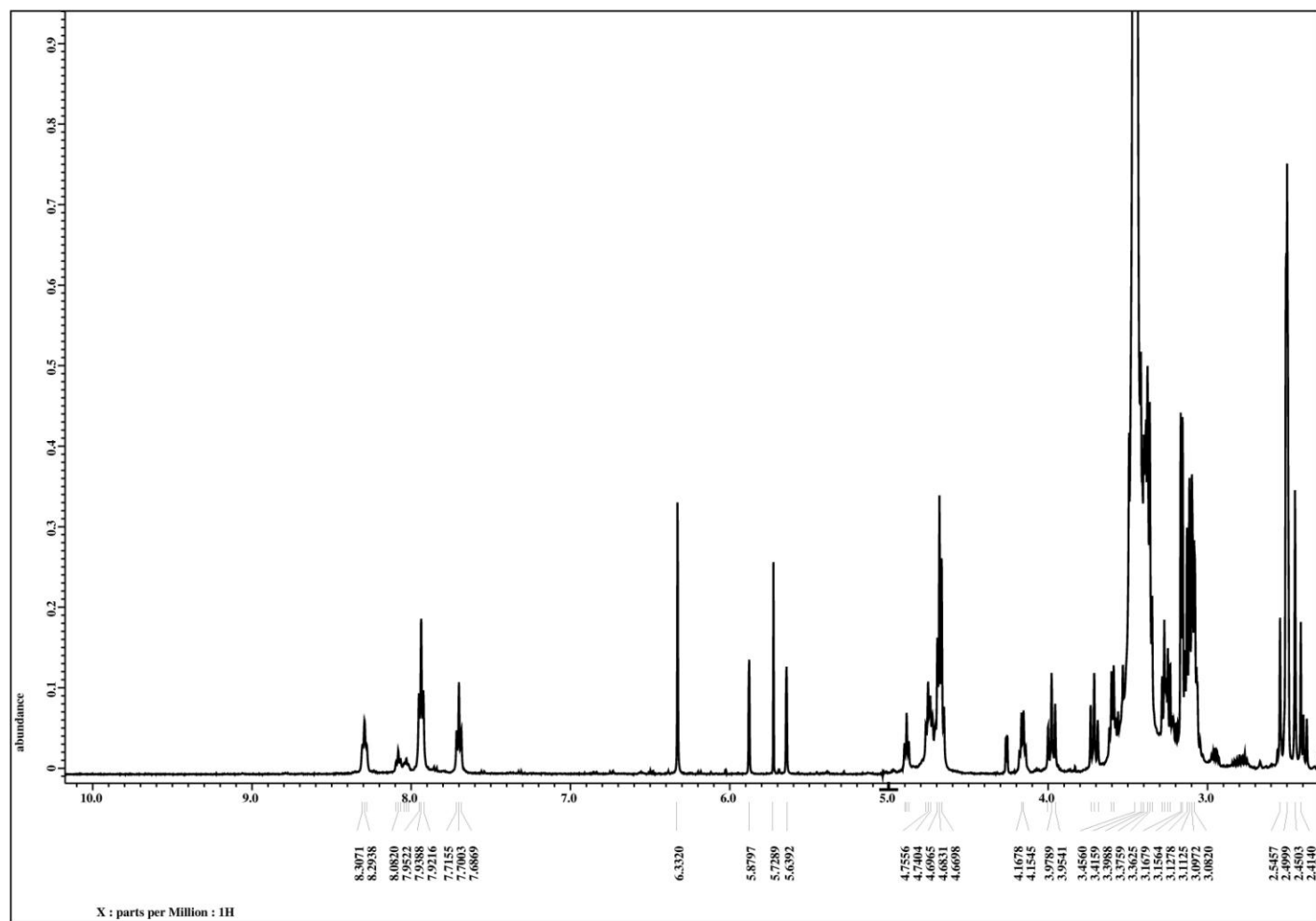


Figure S1. ^1H NMR spectrum of CD in DMSO-d_6 .

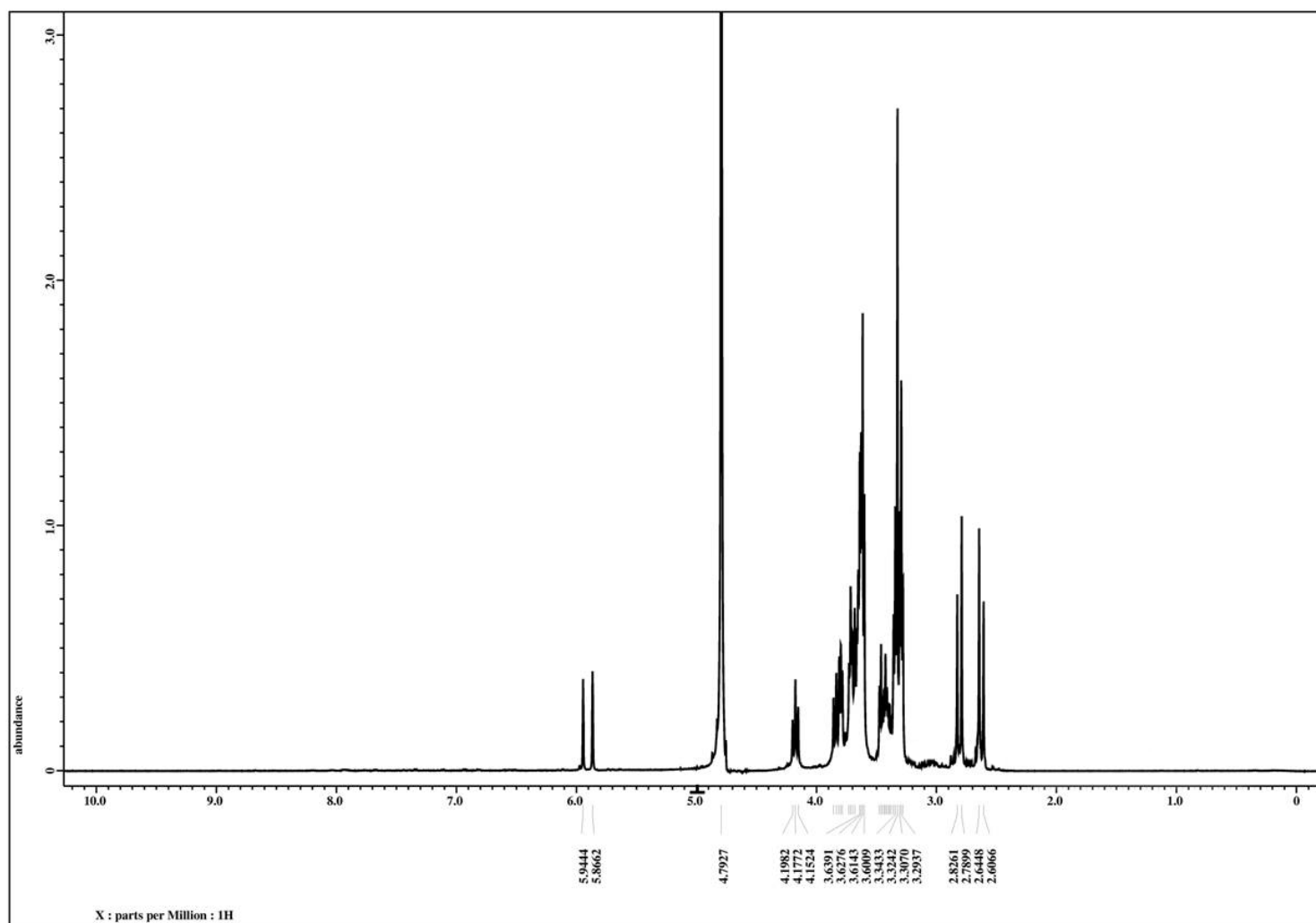


Figure S2. ^1H NMR spectrum of CD in D_2O .

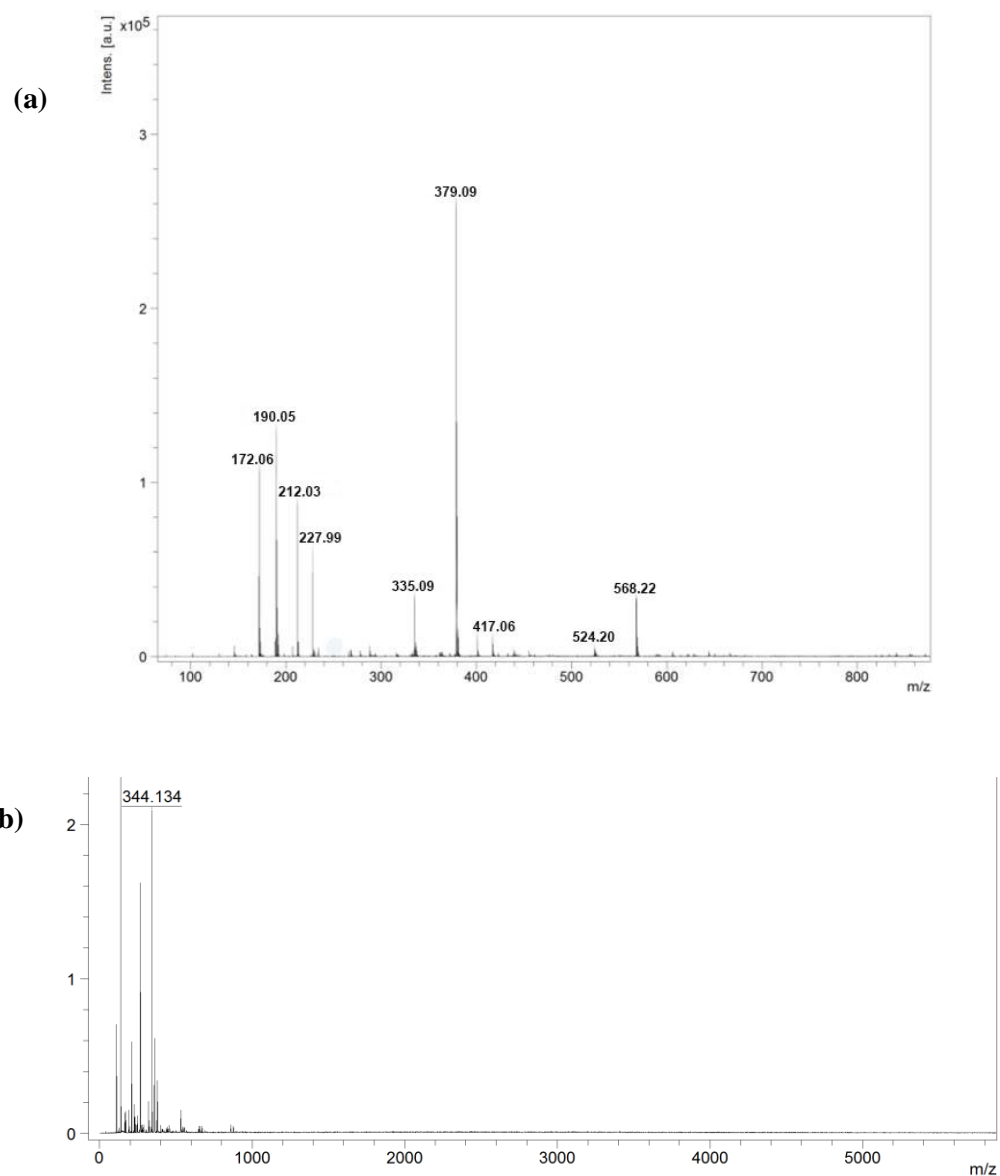


Figure S3. MALDI mass spectrum of CHCA Matrix (a), MALDI mass spectrum of CDs with CHCA matrix (b).

Table S1. m/z values in MALDI mass

	m/z values
CHCA matrix	172.06, 190.05, 212.03, 227.99, 335.09, 379.09, 417.06, 524.20, 568.22
CDs with CHCA matrix	172.06, 212.03, 227.99, 249.99, 268.11, 286.10, 322.16, 344.13, 360.11 , 379.09, 568.20

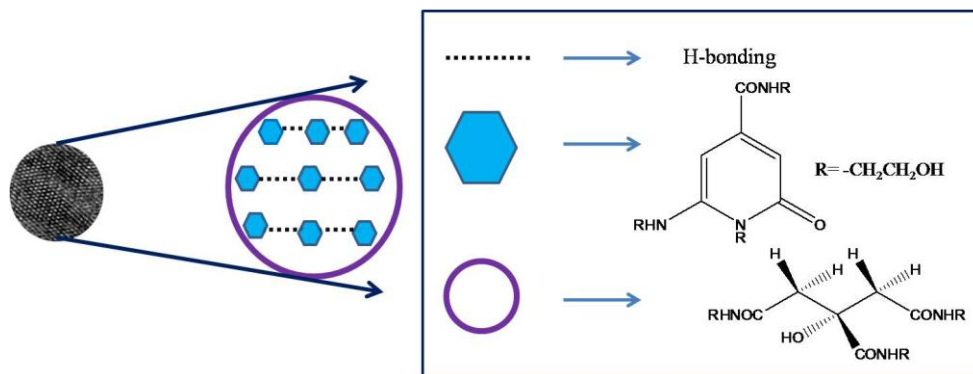


Figure S4. Formation of CD by stacking of fluorophores.

AFM experimental details and image.

The morphology of carbon dot was investigated by atomic force microscopy. Atomic force microscopy was carried on NT-MDT (model no. AP-0100) in semicontact mode. The carbon dot was dissolved in methanol and drop casted on a microscopic glass coverslip.

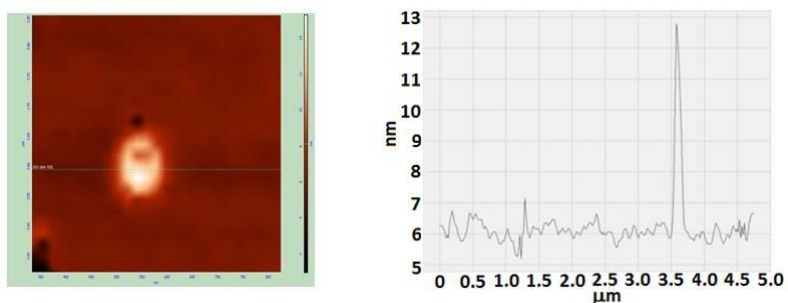


Figure S5. AFM image and its corresponding size of CD.



Figure S6. Inverted round-bottomed flask showing gel nature of CD.

Computational calculation of 2-pyridone derivative.

The geometry of the molecule has been optimized by density function theory (DFT) using Gaussian 09 software [S1]. All the calculations were performed using B3LYP functional and 6-31G basis set for all the atoms. Default criteria for geometry optimization were used in each case.

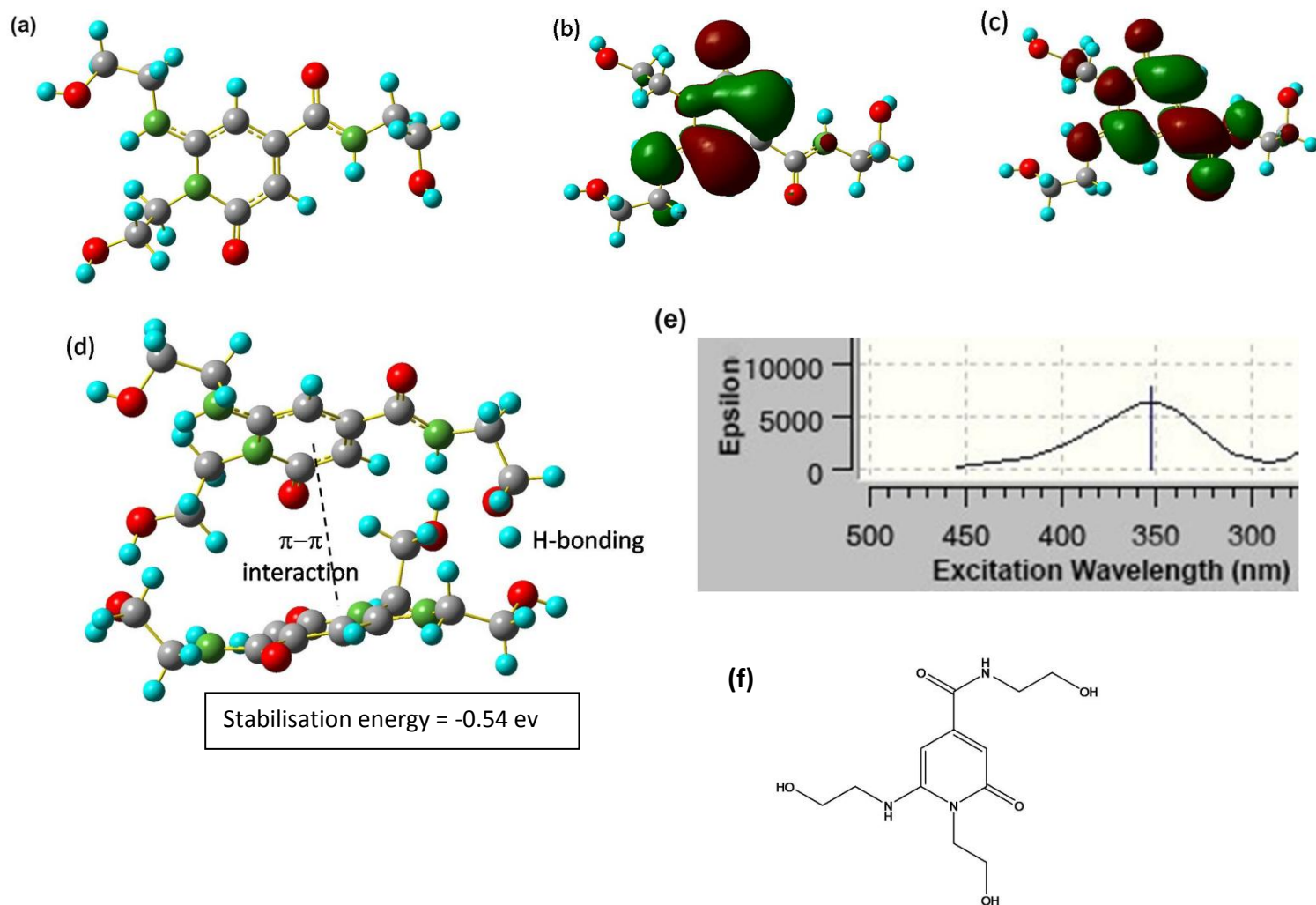


Figure S7. Geometry optimized structure (a), orbital picture of HOMO (b), LUMO (c) of 2-pyridone derivative. Stabilisation due to π - π interaction and H-bonding (stabilisation energy = -0.54 eV) has been shown in between two 2-pyridone derivatives (d). Computational UV-VIS spectrum of 2-pyridone derivative (e). Structure of 2-pyridone derivatives (f).

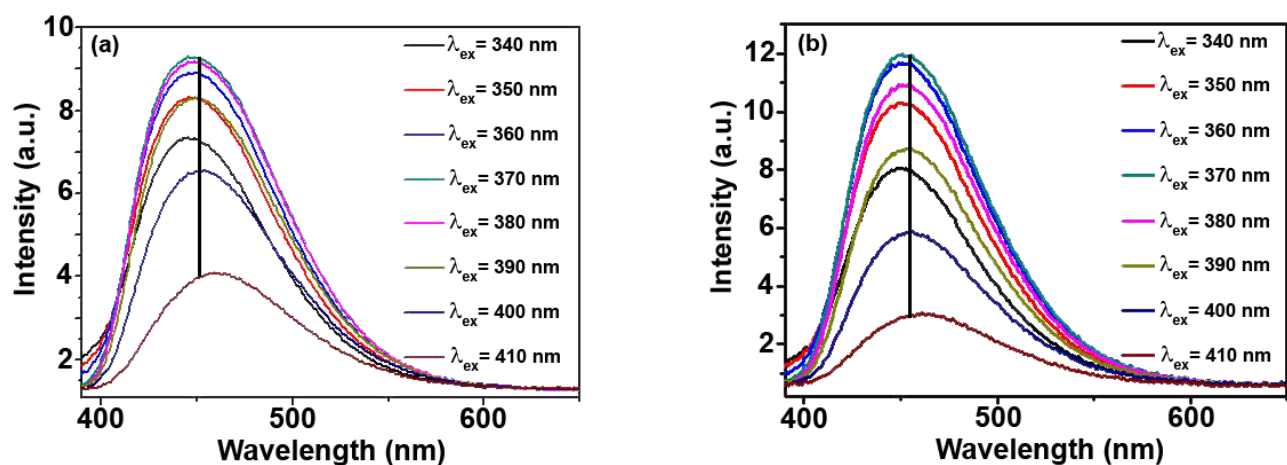


Figure S8. Emission behavior of CD in acetonitrile (a) and methanol (b).

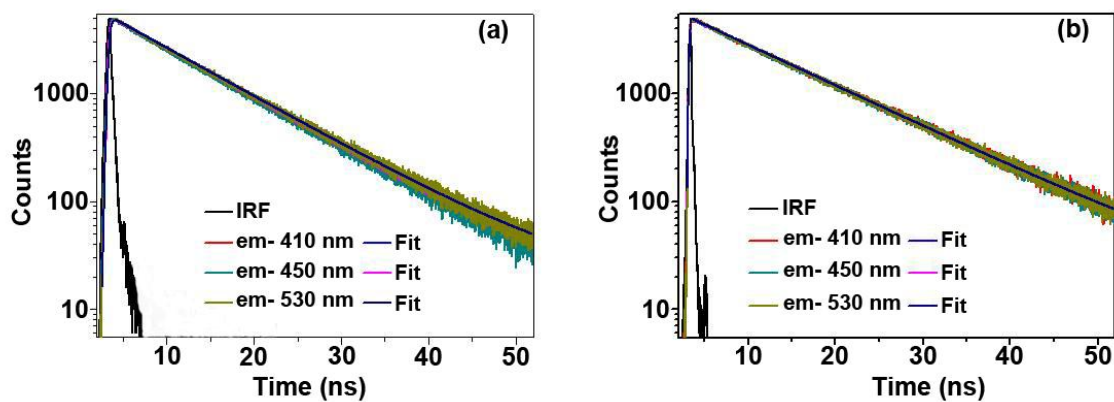


Figure S9. TCSPC decay of CD in acetonitrile (a) and methanol (b).

Photostability experiment:

Procedure for photostability measurement:

For photostability measurement 25 mL stock solutions of carbon dot (in water), CdSe QD (in toluene), and CdSe/CdS QD (in toluene) were kept in three different glass vials (volume = 30 mL) and put in a UV chamber. Absorbance of each solution of carbon dot, CdSe QD and CdSe/CdS QD were kept in between 0.18 to 0.20 at the irradiation wavelength (360 nm) (see figure below). Three stock solutions were continuously irradiated with two 360 nm 8 W each UV lamps. The distance between UV lamp and the top of each glass vial was 10 cm.

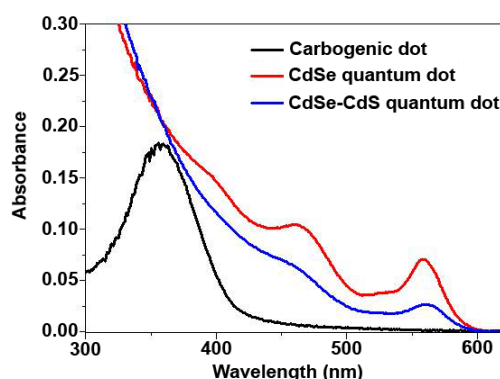


Figure S10. Absorption spectra of carbon dot, CdSe QD, and CdSe/CdS core-shell QD.

Synthesis of QD.

CdSe core was synthesized following a literature procedure using ‘hot injection’ method [S2]. TOPO was used as a ligand. CdSe QDs were purified by centrifugation and decantation and then dispersed in toluene for further processing. CdSe/CdS core/shell QDs were prepared by SILAR (Successive Ion Layer Adhesion and Reaction) technique following a literature procedure [S3,S4]. Oleic acid was used as a ligand. Both the CdSe-core and CdSe/CdS core/shell QDs were synthesized in Schlenk line setup to maintain standard air free atmosphere. All chemicals required for the synthesis of QD were procured from Sigma-Aldrich.

pH dependent experiment:

All the solutions (from pH 2 to pH 12) were prepared and checked by using a bench top pH meter (SESHIN, ECM-710). A fixed amount of CD was dissolved in all pH solutions ($\sim 4 \mu\text{g}$ in 2.5 mL). Absorption spectra were recorded in Carry 300 Bio UV-VIS spectrophotometer.

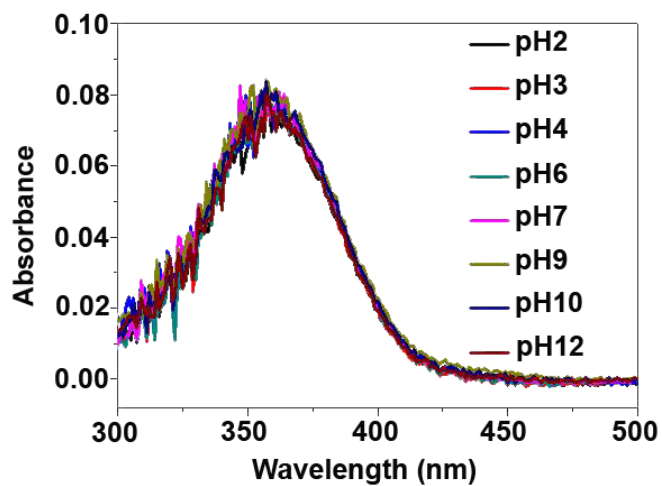


Figure S11. Absorption spectra of CD at different pH.

Single particle movie:

A movie showing the gradual decrease of PL intensity of CD at the single particle level.



Movie_Final.avi

References

- [S1] Frisch, M. J.; Trucks, G. W.; Schlegel, H. B.; Scuseria, G. E.; Robb, M. A.; Cheeseman, J. R.; Scalmani, G.; Barone, V.; Mennucci, B.; Petersson, G. A., et al. Gaussian 09, Revision D.01; Gaussian, Inc., Wallingford, CT, 2009.
- [S2] Aldana, J.; Wang, Y. A.; Peng, X. G. Photochemical Instability of CdSe Nanocrystals Coated by Hydrophilic Thiols. *J. Am. Chem. Soc.* **2001**, *123*, 8844-8850.
- [S3] Li, J. J.; Wang, Y. A.; Guo, W. Z.; Keay, J. C.; Mishima, T. D.; Johnson, M. B.; Peng, X. G. Large-Scale Synthesis of Nearly Monodisperse CdSe/CdS Core/Shell Nanocrystals Using Air-Stable Reagents via Successive Ion Layer Adsorption and Reaction. *J. Am. Chem. Soc.* **2003**, *125*, 12567-12575.
- [S4] Xie, R.; Kolb, U.; Li, J.; Basche, T.; Mews, A. Synthesis and Characterization of Highly Luminescent CdSe-Core CdS/Zn_{0.5}Cd_{0.5}S/ZnS Multishell Nanocrystals. *J. Am. Chem. Soc.* **2005**, *127*, 7480-7488.